Journal Name

Preprint submitted to J. Mater Chemistry 2015.

Dynamic Article Links ►

Cite this: DOI: 10.1039/c0xx0

www.rsc.org/xxxxxx

ARTICLE TYPE

VO_2F: a new transition metal oxyfluoride with high specific capacity for Li ion batteries

Juan Carlos Pérez-Flores[a], Raquel Villamor[b], David Ávila-Brande[b], José M. Gallardo Amores[c], Emilio Morán[b], Alois Kuhn[a] and Flaviano García-Alvarado[a,*]

Received (in XXX, XXX) Xth XXXXXXXXX 20XX, Accepted Xth XXXXXXXXX 20XX
DOI: 10.1039/b000000x

Hitherto unreported vanadium oxyfluoride VO_2F has been synthesized using a solid state reaction at pressures of 4 GPa and 800 ºC. This long awaited vanadium oxyfluoride fills the existing gap of ReO_3-type MO_2F compounds of Group 5 elements, from which only NbO_2F and TaO_2F were known to exist to date. VO_2F crystallizes with the VF_3-type structure, space group *R*-3*c*, with a = 5.1226(1) Å, c = 13.0686(3) Å as determined by powder X-ray diffraction. Highly structured diffuse streaking observed in electron diffraction patterns evidences local O/F ordering. VO_2F exhibits two regions upon discharge in a lithium cell, an upper sloped region in the range 3.9-2.2 V and a lower plateau at 2.15 V. Discharge of VO_2F to 1 V provides a gravimetric capacity of 450 mAh g^{-1}. VO_2F can reversibly insert up to 1 Li^+ per vanadium above 2.15 V without destruction of the host structure, delivering a gravimetric capacity as high as 250 mAh g^{-1} and pointing to VO_2F as a promising intercalation electrode.

Introduction

After intensive investigation of light transition metal (TM) oxides as electrodes for lithium ion rechargeable batteries, new chemistries based on different ligands are needed to fulfill performance demands for superior energy storage devices. Oxyfluorides have been capturing attention lately in the search for superior electrodes.[1] The partial substitution of oxygen with fluorine in the structure could offer a higher average electrode potential. The expected increase of the intercalation potential should be high enough to get a significant increase of specific energy without exceeding the high voltage stability limit of the commonly used liquid electrolytes. On the other hand, crystal chemistry of oxyfluorides may provide crystalline structures with relevant topotactical features for lithium intercalation, in which lithium diffusion paths provided by the different structures allow for a relatively fast ionic conduction. Lithium diffusion may occur along one, two or three spatial directions depending on the particular host structure. In the case of 1-D Li diffusion the existence of defects, blocking the diffusion path, limits the performances of the intercalation electrode. That is the reason why 2-D or 3-D hosts are preferred.

Among manifold 3D-hosts, the well-known ReO_3 structure type has been reported as attractive lithium insertion host for several first-row TM trioxides (TM=Mo, W, Re)[2-10] and trifluorides (TM=Ti, V, Cr, Fe)[11-14], though some of the latter cases have been found to be more interesting as convertibles compounds[11, 14, 15]. It is built up of [Re-O_6] octahedra sharing all corners along the three spatial directions. The interesting topology for lithium intercalation arises from the existence of an empty cube octahedral interstice (joining square anion faces to the next), in which small cations such as lithium can be inserted. However, the preference of lithium for a lower coordination produces a distortion of this cavity, enabling two octahedral empty sites available for lithium instead[2]. ReO_3 itself can insert up to 2 Li^+ per formula, corresponding to the complete filling of both octahedral sites. However, the excessive atomic weight of rhenium and other second or third row TM leads to poor specific capacities. Nevertheless, there is a growing interest in structures able to intercalate 2 Li/TM, and many efforts have been made up to now to use them as electrodes for a lithium ion battery.

Among all oxyfluorides reported so far, only the following three transition metals M = Ti, Nb and Ta (belonging to group 4 and group 5) have been known to crystallize in the ReO_3-type structure, according to compositions MOF_2 (M=Ti) and MO_2F (M=Nb, Ta). Excitingly, only NbO_2F and TaO_2F are known to exist among the elements belonging to the Group 5. In the 1960s Weidlein and Dehnicke reported on a VO_2F compound obtained by direct fluorination of VO_2Cl[16]. However, its IR spectrum suggested the existence of discrete VO_2^+ (point group C_{2v})

[a] *Universidad CEU San Pablo, Facultad de Farmacia, Departamento de Química y Bioquímica, Urb. Montepríncipe, Boadilla del Monte, E-28668, Madrid, Spain. Fax: 34 91 3510496; Tel: 34 91 3724728; e-mail: flaga@ceu.es*
[b] *Universidad Complutense de Madrid, Facultad de Ciencias Químicas, Departamento de Química Inorgánica, Ciudad Universitaria s/n, 28040 Madrid, Spain.*
[c] *Universidad Complutense de Madrid, Facultad de Ciencias Químicas, Laboratorio de Altas Presiones, Ciudad Universitaria s/n, 28040 Madrid, Spain.*

Electronic Supplementary Information (ESI) available: [**Fig. SI 1** EELS spectrum of VO_2F showing the V-$L_{2,3}$; O-K and F-K ionization edges; **Fig. SI 2** Cycling behaviour of a half lithium cell bearing VO_2F as the electrode active material in the 3.9-2.2 V range at C/50; **Fig. SI 3.** dx/dE for VO_2F at room temperature. The first three cycles of a lithium half cell are shown.]. See DOI: 10.1039/x0xx00000x

oxocations and F^- ions[17]. Notably, and much to our surprise, a ReO_3-type VO_2F has not been synthesized to date. Interestingly, the oxyfluorides $TiOF_2$ and NbO_2F are able to reversibly insert 0.38 Li (2.5-0.9V range) and 0.54 Li (2.5-1.4 V range) respectively per TM, with a capacity of 100 mAh g^{-1} for both[18-22]. Deep discharge of these oxyfluorides in lithium cells triggers the destructive conversion of the pristine material.[19, 22] The $TiOF_2$ structure is destroyed between 0.8-0.9 V, delivering a total capacity of 750 mAh g^{-1} after complete reduction down to 0.005 V. The composite Li_xTi-LiF formed is able to sustain a capacity of 400 mAh g^{-1} in the 0.005-3 V range, showing the characteristic behavior of convertible compounds. The presence of Nb^{5+} in NbO_2F is appealing for lithium intercalation reactions. However, the high molecular weight is a major drawback for its use in batteries. The general electrochemical reactivity with lithium upon reduction at low voltage was similar to that observed for $TiOF_2$, with destruction of the crystalline structure[19, 22, 23]. The long voltage plateau at 1.4 V was assigned to the destruction of the structure, producing the amorphization of the active material[18, 19, 21, 23]. The total capacity delivered down to 0.005 V reached 660 mAh g^{-1}, from which 296 mAh g^{-1} are recovered on charge.

In view of these results we were wondering if hitherto unknown VO_2F would be an interesting electrode material. The reduction of V^{5+} offers a higher capacity while maintaining intact the electrochemical activity within the stability potential window of the electrolyte. Owing to the lightness of V, a substantial benefit of specific capacity is expected when compared to NbO_2F. This work is in part a continuation of our ongoing investigations addressed to synthesize new oxide-fluoride phases. As a very interesting example, the existence of VO_2F is reported for the first time. In this work we report on the synthesis of unknown vanadium dioxyfluoride VO_2F and fill hereby the present gap for MO_2F compounds of Group 5 elements. We herein describe the synthesis procedure to obtain VO_2F. Chemical composition of vanadium dioxyfluoride has been determined combining elemental analysis and WDS, while double redox titration and EELS was used to confirm the high oxidation state of vanadium. We have further investigated the structure, microstructure and the electrochemical Li insertion properties of VO_2F. Our electrochemical results point to VO_2F as an outstanding new battery material regarding specific capacity and reversibility of the intercalation reaction. Herein we demonstrate that the new vanadium dioxyfluoride VO_2F can reversibly insert up to 1 Li^+ per TM delivering a capacity as high as 250 mAh g^{-1}.

Experimental Section

VO_2F samples were prepared through a high pressure procedure. V_2O_5 (Aldrich, 99.9%) and VOF_3 (Aldrich, 99%) were finely ground and mixed in a 1:1 molar ratio, according to the reaction:

$$V_2O_5 + VOF_3 \rightarrow 3\ VO_2F \qquad \textbf{(1)}$$

The mixture was put in a gold capsule. All operations were performed in an argon-filled glove box to avoid exposure to oxygen or moisture, given the hygroscopic characteristic of VOF_3. The gold capsule was transferred to a CONAC press working in the 2-5 GPa pressure and 773-1123 K range. Pressure was calibrated with metallic Bi. Several experiments were performed at different pressure and temperature in order to find the optimal synthesis conditions. Samples were held at 4-5 GPa and 973-1073 K for 30 min, quenched under pressure, decompressed for 1 h and recovered to ambient conditions.

Sample purity was checked by powder X-ray diffraction (XRD) using a Bruker D8 high-resolution diffractometer, with monochromatic $CuK_{\alpha 1}$ (λ = 1.5406 Å) radiation, obtained with a germanium primary monochromator and equipped with a position sensitive detector (PSD) MBraun PSD-50M. The same equipment was used to characterize the products synthesized by electrochemical methods (see below). An air-tight sample holder was used for characterization of electrochemically intercalated/deintercalated materials to avoid contact with atmosphere.

Elemental analysis to quantify oxygen and fluorine contents was carried out by Wavelength Dispersive Spectroscopy (WDS) using a JEOL Superprobe JXA-8900 M apparatus operated at 15 KV and 20 nA. The beam width was kept in the 5-10 micrometer width range in order to minimize loss of fluorine. LIFH and LDE1 crystals were used for the analysis of O and F respectively. The oxidation state of V in the compound was determined by two independent techniques. On one hand, double redox titration following the procedure described by Hodnett *et al.*[24] V_2O_5 (Aldrich, 99.9%) was also analyzed as a reference. On the other, electron energy loss spectroscopy (EELS) using a transmission electron microscope (see below).

For transmission electron microscopy (TEM) studies samples were ground in *n*-butyl alcohol and ultrasonically dispersed. A few drops of the resulting suspension were deposited on a carbon-coated grid. The study of the reciprocal space by selected area electron diffraction (SAED) was carried out in a JEOL JEM2100 microscope operating at 20kV with a double tilt (±45°) goniometer. High resolution transmission electron microscopy (HRTEM) and electron energy loss spectroscopy (EELS) experiments were performed with a JEOL JEM 3000F microscope operating at 300 kV (double tilt (±20°) point resolution 0.17 nm), fitted with an energy-dispersive X-ray spectroscopy (XEDS) microanalysis system (OXFORD INCA) and ENFINA spectrometer with an energy resolution of 1.3 eV.

Electrochemical characterization of VO_2F was performed in CR2032 coin cells. The positive electrode was prepared from VO_2F powder manually mixed with carbon black (C-NERGY Super C65, Timcal) and a binder agent (Kynarflex) in a 75:20:5 weight ratio and dried at 70ºC. Additionally, some other electrodes were prepared from ball milled samples at 15 Hz for 1.5 h using a mixer mill MM 301 (Retsch) with two jars (10 ml) and grinding balls of tungsten carbide to grind and homogenize the sample by impact and friction.

Pellets of 8 mm diameter and containing typically 13-16 mg of sample were conformed from this mixture by uniaxial pressing. A lithium foil was used as the negative electrode, while a 1M $LiPF_6$ solution in EC:DMC (1:1) was used as the electrolyte (LP30, Selectilyte G1, BASF). Cells were run using a MacPile II system. Galvanostatic experiments were carried out at a constant current of C/50 (this is insertion/deinsertion of 1 Li in 50 h) to characterize the electrode material. Electrochemical synthesis of samples suitable for *ex situ* XRD characterization was made by

potentiostatic discharge/charge; cells were discharged or charged to at a determined voltage and left to equilibrate until the measured current was < 1 μA. Cells were then stopped and the pellets subjected to XRD analysis.

Discussion

Chemical and structural characterization

Examination of the XRD patterns confirms the synthesis of a polycrystalline product at 4 GPa and 1073K, afterwards quenched to room temperature, that adopts the rhombohedral VF_3-type structure[25]. In addition, only a small amount (ca. 3 %) of an unknown impurity is observed. Thus we assumed these conditions as optimal synthesis conditions of VO_2F. Pattern analysis resulted in the following hexagonal lattice parameters: $a = b = 5.1226(1)$ Å, and $c = 13.0686(3)$ Å (space group $R\text{-}3c$). Lattice parameters are compared to other group 4 and group 5 TM oxyfluorides in Table 1.

TABLE 1: New VO_2F and other known TM oxyfluorides crystallizing in the ReO_3-type structure

Group 4		**Group 5**	
$TiOF_2$	*Pm-3m* a = 3.798(5) Å [25] *R-3c* [26] a = 5.3325(1) Å, c = 13.2321(4) Å	**VO_2F**	*R-3c* (this work) a = 5.1226(1) Å, c = 13.0686(3) Å
$ZrOF_2$	(structure not determined) [27]	NbO_2F	*Pm-3m* a = 3.899(2) Å [28] *R-3c* (high pressure form*) [29] a = 5.3067(4) Å, c = 13.5495(8) Å
		TaO_2F	*Pm-3m* a = 3.896(3) Å [30]

* at 1.38 GPa

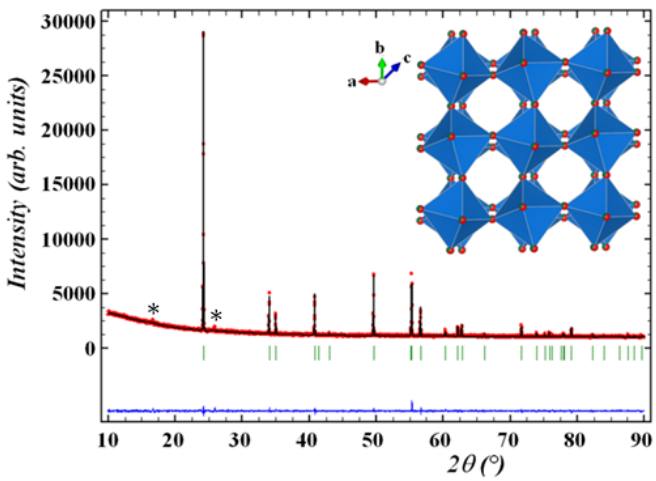

Fig. 1 Final observed (points) and calculated (solid line) X-ray diffraction profile (λ = 1.5406 Å) for VO_2F at 298 K ($a = b = 5.1226(1)$ Å, and $c = 13.0686(3)$ Å, space group $R\text{-}3c$). Peaks marked with asterisks come from the presence of a small amount (ca. 3%) of an unknown impurity. Inset shows the three dimensional packing of VO_2F. Vanadium oxide fluoride octahedra are blue.

The final reliability parameters are *R*p = 2.96 %, *R*wp = 3.83 %, *R*Bragg = 3.67 % and χ^2 = 1.91. Experimental and calculated X-ray diffraction pattern are given in Figure 1. The main structural parameters of the refinement are summarized in Table 2.

TABLE 2: Atomic positions, isotropic thermal displacement, occupancies, interatomic distances and angles determined by powder XRD (T = 298 K) for VO_2F with space group *R-3c*.

Atom	**Site**	**x**	**y**	**z**	**Occ**	**U_{iso}**
V	6b	0	0	0	1.0	0.0206(9)
O	18e	0.5811(2)	0	¼	0.67	0.076(1)
F	18e	0.5811(2)	0	¼	0.33	0.076(1)
Atomic distances (Å) and angles (º)						
d(V-O/F)	1.883(2) x 2; 1.883(3) x 2; 1.883(8) x 2					
d(O/F–O/F)	2.661(2); 2.661(4) x 2; 2.661(6) x 2; 2.665(2); 2.665(3); 2.665(8)					
V-(O/F)-V	154.5(1)					

The final Rietveld refinement shows that the three-dimensional framework of VO_2F is built up of corner sharing almost regular V-$(O/F)_6$ octahedra (Fig. 1), derived from cubic ReO_3, but with an $a^-a^-a^-$ tilting of octahedra from the cubic axis. Oxygen and fluorine atoms are randomly distributed in the nonmetal 18*e* position. Each O/F anion is coordinated with two V^{5+} to form zigzag-like infinite V−(O/F)−V chains, with a V−O/F−V bending angle θ = 154.5(1)° and a rotation angle of $V(O/F)_6$ octahedra from the cubic axis φ = 15.6(1)º. These angles are similar to those detected in VF_3 (θ = 149.1(1)° and φ =18.9(1)º) [25]. The V-(O/F) distance of 1.883 Å is between that of the average V-O distance (1.825 Å) in V_2O_5 [26] and the average V-F distance (1.938 Å) found in VOF_3 [27], in agreement with the mixed anion structure.

The average VO_2F structure has been subjected to bond length-bond valence analysis[28]. Apparent valence (AV) calculations indicate that oxygen, with AV = 1.661, is significantly underbonded in the single random anion position whereas fluorine, with AV = 1.253, is significantly overbonded. Using the two R_0 bond valence parameters reported: $R_0(O)$ = 1.803 Å and $R_0(F)$ = 1.71 Å [28], the calculated V^{5+} - anion distance would be 1.803 Å when O^{2-} is the anion, but it would be 1.966 Å when F^- is the anion. The experimentally determined V^{5+} - anion separation, 1.883 Å in VO_2F, is equidistant in between. These findings suggest short range O/F ordering, as reported for other TM oxyfluorides[29-31]. This could be furthermore linked to the increased value of isotropic thermal displacement parameter for the V site (U=0.0206(9) $Å^2$), as determined from our structural

refinement.

The morphology of the as prepared VO_2F is shown in Figure 2a. Very large particles from 1 to 60 μm are obtained. However, the existence of smaller particles, agglomerated to the larger ones, indicates a broader particle size distribution.

Preliminary chemical analysis carried out by EDS revealed the presence of both oxygen and fluorine. Quantification of oxygen and fluorine by means of WDS confirmed the O/F ratio to be close to 2. Double redox titration yielded an average vanadium oxidation state of +4.98, in agreement with the proposed VO_2F formula. Interestingly, the small amount of V^{4+} is important to provide electronic conductivity and explains the dark brown color of the as prepared sample. Thus, the existence of a solid solution $VO_{2-x}F_{1+x}$ ($V^{5+}_{1-x}V^{4+}_{x}O_{2-x}F_{1+x}$) can be admitted. In any case, just for simplicity and owing to the small amount of V^{4+}, we will refer to the obtained sample as VO_2F.

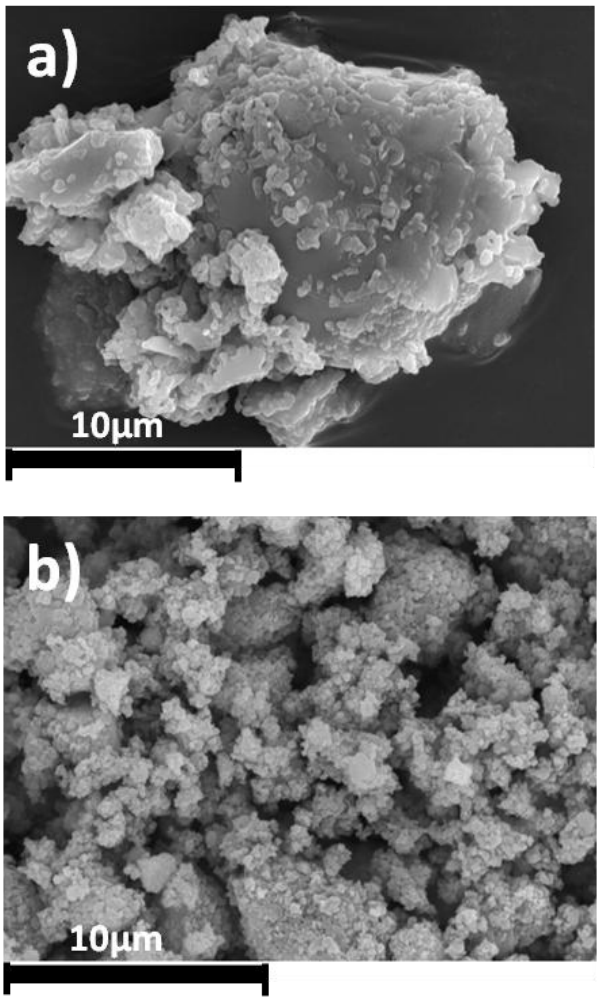

Fig. 2 Low magnification SEM images showing the typical shape and size of a) as prepared VO_2F by high pressure synthesis and b) after processing by ball milling for 1 hour.

Electron energy loss spectroscopy (EELS) is a powerful technique to identify the different elements present in a material as well as to confirm the oxidation state of transition metals. The EEL spectrum of VO_2F, recorded between 500 and 750 eV (see Supporting Information Figure SI 1) shows the characteristic edges (V $L_{2,3}$; O K and F K) of the elements. However due to the strong overlapping between V $L_{2,3}$ and O K edges a realistic quantification of the light elements (F and O) cannot be carried out. Nevertheless, if the ratio O/F in the material is 2:1 the oxidation state of vanadium must be 5+.

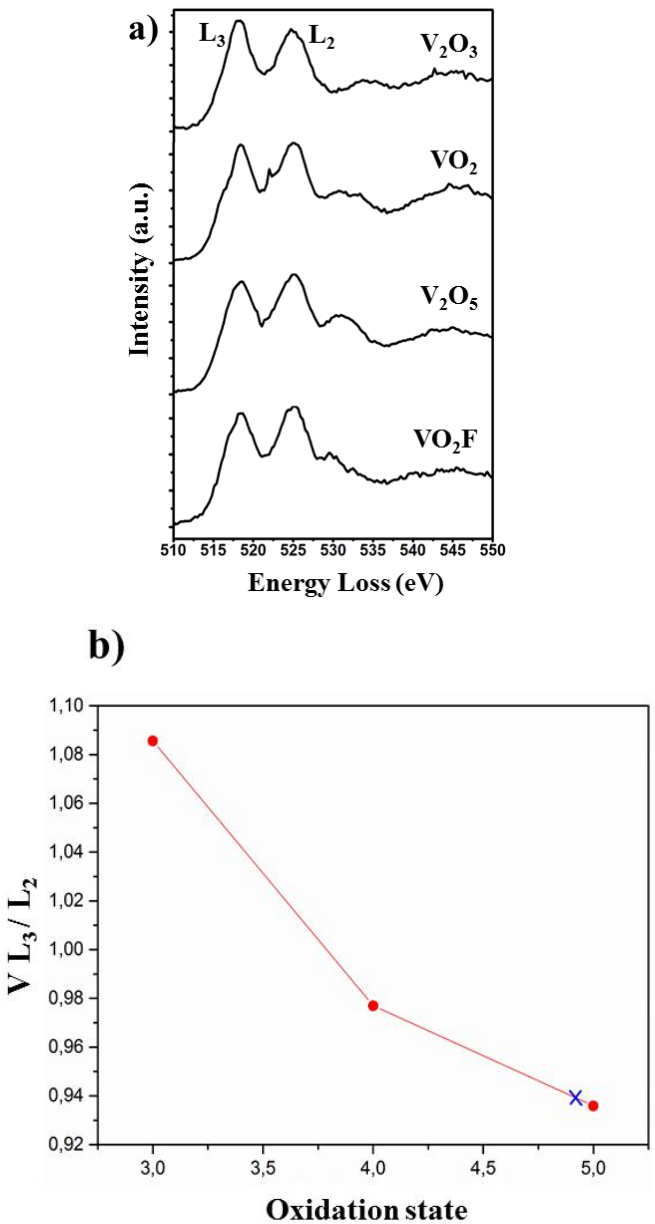

Fig. 3 a) Experimental $VL_{2,3}$ electron energy loss spectra taken from bulk V_2O_3, VO_2, V_2O_5 and VO_2F, b) Graphic representation of L_3/L_2 intensity ratio versus vanadium oxidation state in standard V oxides and in the studied material (blue cross).

Since the oxidation state of V can be determined by EELS, vanadium $L_{2,3}$ edge fingerprints for V^{3+}, V^{4+}, and V^{5+} were established from bulk reference samples (V_2O_3, VO_2 and V_2O_5) and used for the characterization of VO_2F. As it can be observed in Figure 3a, there is a modification of the intensity ratio of L_3/L_2 edges related to the oxidation state of vanadium. In V_2O_3 (V^{3+}) the intensity of the L_3 edge is slightly higher than L_2, but the

increase of the oxidation state provokes similar intensities of both edges in VO_2 (V^{4+}). Finally in V_2O_5 (V^{5+}) the situation is inverted in comparison to V_2O_3 showing in this case the L_2 edge a slightly higher intensity[32]. We can make use of this observation to quantify the oxidation state of vanadium in VO_2F by building up a calibration graph relating oxidation state and the ratio of the white line intensity ratio L_3/L_2 (Figure 3b), as it has been described for other transition metals.[33] The intensity ratio obtained for VO_2F gives an average oxidation state for V of +4.93, very close to the expected value for a composition VO_2F and in full agreement with the value obtained by double redox titration (+4.98).

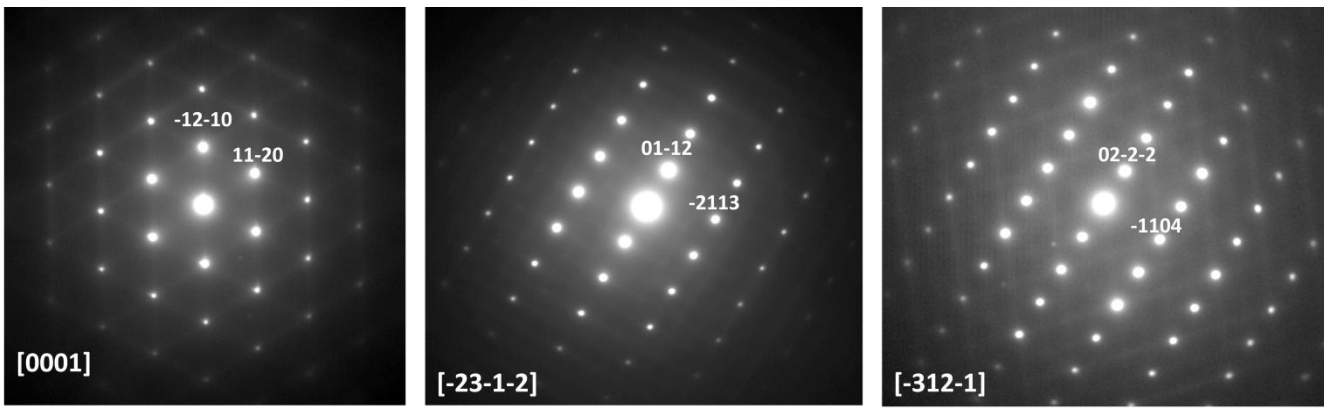

Fig. 4 SAED patterns of VO_2F recorded along [0001], [-23-1-2] and [-312-1] zone axes. Note in each pattern the diffuse streaking lines produced by the local order between O/F.

Microstructural characterization

To further characterize vanadium oxyfluoride, the microstructure has been investigated. The study of the reciprocal space of VO_2F by electron diffraction shows extra features in the form of lines of diffuse streaking lines in addition to the basic reflections (see Figure 4). The last were indexed on the base of the hexagonal unit cell, space group *R*-3*c*. The existence of a highly structured diffuse intensity distribution in the form of continuous rods evidences a local ordering of oxygen/fluorine in the present material, as it has been previously detected in other $MO_{3-x}F_x$ (M = Nb, Ta, Ti, Mo, W) with ReO_3 type structure[29]. For several TM oxide fluorides $[MOF_5]^{2-}$, the formation of a short M-O bond, which leaves a long trans M-F bond, is correlated with an off-center shift of the central cation, resulting in distortion of the octahedron[34]. A closer investigation of the microstructure of VO_2F has been performed by HRTEM. In Figure 5 the structural projections along the main orientations are depicted. The darker contrast represents the atomic arrangement of the vanadium framework, evidencing the absence of extended defects. However, the mottled contrast clearly observed in all the images corresponds to the short range order between F/O around the interconnected octahedra, which is also detected as a diffuse scattering in the Fast Fourier transforms displayed as insets in the images.

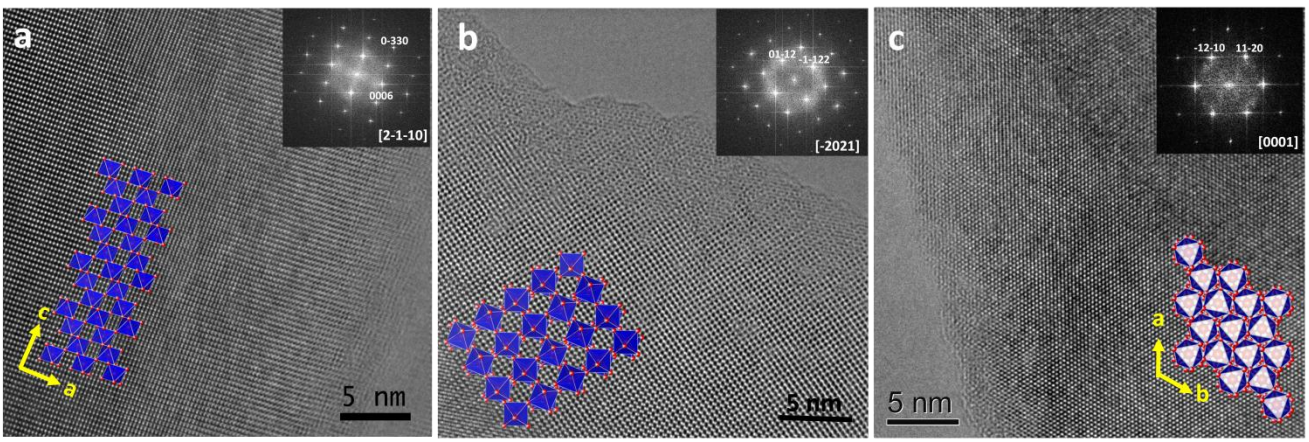

Fig. 5 HRTEM images of VO_2F along (a) [2-1-10], (b) [-2021] and (c) [0001] zone axes (the projected structural models are not in scale to the experimental images).

Electrochemical lithium insertion

As in the case of VF_3 the topology of VO_2F is adequate for intercalation reactions, but for the latter the presence of pentavalent vanadium enables lithium intercalation, therefore the electrochemical properties of vanadium oxyfluoride have been tested against lithium metal. The galvanostatic discharge curve (Figure 6) of the as prepared compound in the range 3.9-1 V exhibits two regions, an upper sloped region, in the range 3.9-2.2 V, followed by a lower plateau at 2.15 V. When cycling the cell between 3.9 and 2.2 V an essentially constant capacity of 90 mAh g^{-1} (0.35 Li^+ per TM) is delivered (Figure 7a).

As kinetic limitation owing to the big particle size (Figure 2a) may be at the origin of the moderate capacity delivered in the range 3.9-2.2 V, a sample was ball milled for 1 hour at 15 s^{-1}. On the other hand, electronic limitations are not expected as in fact the presence of a small amount of V^{4+} as determined by EELS likely enhances electronic conductivity. The SEM images shown in Figure 2a and b confirm that ball-milling process contribute to disaggregate and homogenize the sample. More interestingly crystal size of the VO_2F compound is substantially reduced after milling, with a size of most particles < 1 μm. Thus, the gravimetric capacity can be notably enhanced to 250 mAh g^{-1} (1 Li^+ per TM) by this simple optimization process (Figure 7b).

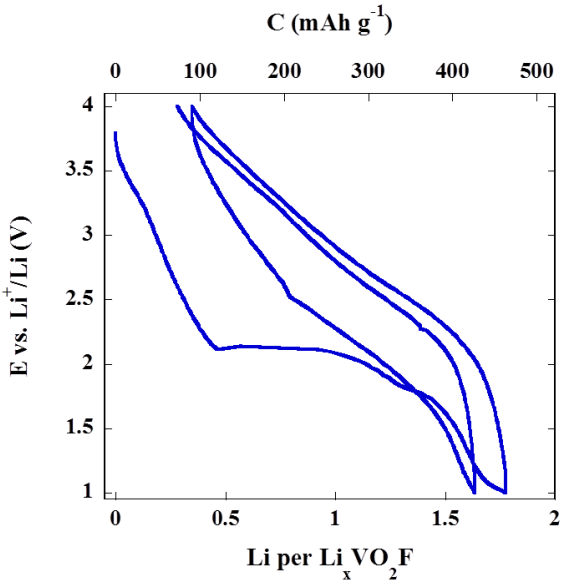

Fig. 6 Galvanostatic curves of as prepared VO_2F in the 3.9-1 V range.

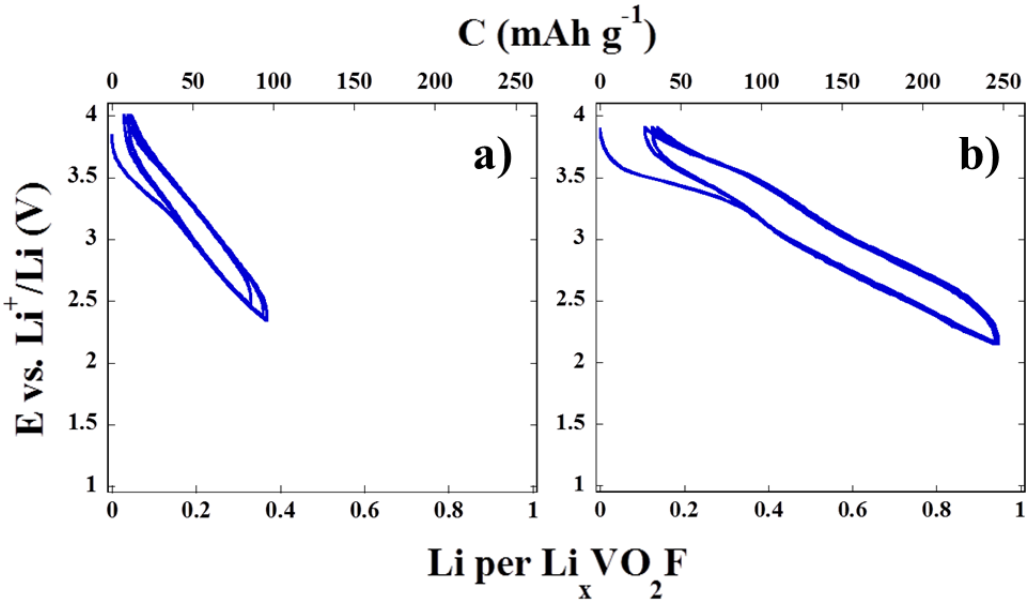

Fig. 7 Galvanostatic discharge-charge curves of VO_2F in the 3.9-2.2 V range at C/50; a) pristine and b) ball milled VO_2F (electrolyte: 1 M $LiPF_6$ in 1:1 EC/DMC). The three first cycles are shown.

The *ex situ* XRD study performed during the discharge of ball milled VO_2F in the same voltage range (3.9-2.2 V) confirms the existence of a topotactic single phase Li insertion mechanism, with only slight changes of hexagonal lattice parameters (Figure 8). Small volume change (less than 0.34%) upon intercalation of ca. 1 lithium/f.u. is noteworthy since such type of material near to zero strain behaviour are desired for long life cycling. Full performances of VO_2F in lithium batteries including the influence electrode processing, synthesis conditions, current rate, electrolyte, etc... will be reported elsewhere.

The general electrochemical behaviour of VO_2F seems to be similar to that reported for NbO_2F[18, 19, 22, 23]. However, the capacity delivered in the upper voltage range by means of intercalation (*ocv*-1.4 V) is limited in NbO_2F (75 mAh g^{-1}) while vanadium oxyfluoride develops a really high capacity, ca. 250 mAh g^{-1}.

The reversibility of the lithium intercalation reaction in VO_2F is clearly seen in Fig. 7b. However, a significant decay of capacity is observed for a higher number of cycles (see Supporting Information, Fig SI 2) indicating that optimization of electrode processing and proper selection of electrolyte may be needed to reach competitive electrochemical performances. Contrary to VO_2F, the reversibility of the intercalation reaction in the upper voltage region of NbO_2F has not been proven to date. The reversible reduction of V^{5+} during the first discharge in a lithium cell occurs through three different processes centered at 3.45, 2.8 and 2.5 V (see Supporting Information, Figure SI 3) with the corresponding oxidation peaks on charge. Thus while NbO_2F is useless as lithium battery positive electrode, the latter is a promising high capacity positive electrode worth being investigated deeply.

	a / Å	c / Å	Vol / Å^3
ocv	5.1210(4)	13.073(2)	296.9(1)
Discharged 2.3V	5.1162(9)	13.051(2)	295.9(1)
Charged 3.9 V	5.1190(4)	13.078(2)	296.8(1)
Δinitial-discharge	0.09%	0.17%	0.34%

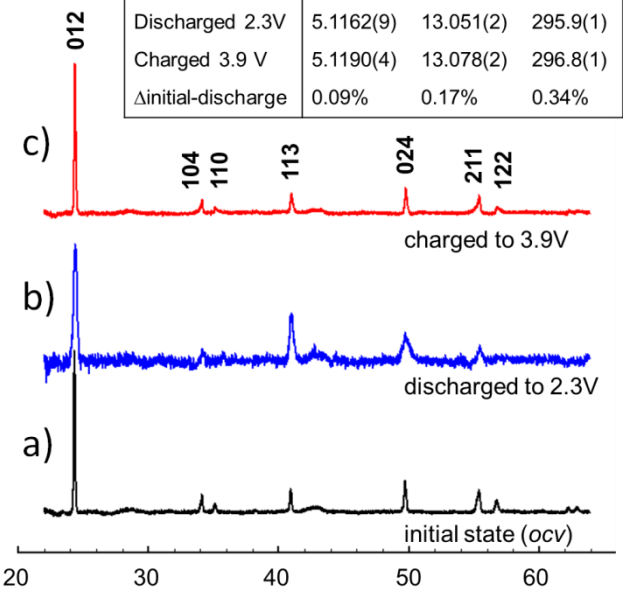

Fig. 8 *Ex situ* evolution of the XRD pattern for the lithium insertion in ball milled VO_2F together with cell parameters of a) initial state (pristine sample), b) discharged (intercalated ca. 1 Li/TM) and c) charged (deintercalated) compound. Inset shows a table with the refined cell parameters and the variation after the first discharge.

For NbO_2F destruction of the structure through a long plateau (at ca. 1.4 V), yielding an amorphous phase was reported. For VO_2F the structure is destroyed along the lower plateau at 2.15 V (Fig. 6) related to an irreversible transformation of the initial compound. Fully discharging a cell to 1 V followed by cycling produces a voltage profile that is different from that of the initial discharge, indicative for an irreversible transformation. At present the origin of lack of reversibility in the V^{5+}/V^{3+} redox couple in VO_2F is not clear. Note that up to $2Li^+$ per TM can be inserted in ReO_3 [2] and 1.3 Li^+ per TM are inserted in the closely related NbO_2F[21], albeit the nature of the highly lithiated phase in the latter case and its structural relationship with the ReO_3 structure has not yet been unveiled.

Conclusions

The most notable point following from our results is that vanadium oxyfluoride VO_2F has been synthesized for the first time, using a solid state reaction at pressures of 4 GPa and temperatures of 800 ºC. VO_2F crystallizes with the VF_3-type structure, space group *R-3c*, with $a = b = 5.1226(1)$ Å and $c = 13.0686(3)$ Å as determined by powder X-ray diffraction. The existence of VO_2F fills the gap of oxyfluorides of Group 5 transition metals with the ReO_3-type structure. Highly structured diffuse streaking observed in electron diffraction patterns evidences local O/F ordering.

Electrochemical discharge of lithium half cells exhibit two regions: i) an upper sloped region in the range 3.9-2.2 V governed by reversible intercalation reaction; ii) a lower plateau region at 2.15 V that points to a conversion reaction. Total discharge of VO_2F to 1 V delivers a gravimetric capacity of 450 mAh g^{-1}. Adjustment of particle size by uncomplicated ball milling has enabled remarkable electrochemical properties. VO_2F is able to deliver up to 1 Li^+ per V in the intercalation range and results to be a promising candidate to high capacity positive electrode for lithium batteries. The gravimetric capacity of 250 mAh g^{-1} is among the highest ever reported for an intercalation compound for the threshold of 1 e^- / formula unit.

Acknowledgements

We thank Ministerio de Economía y Competitividad and Comunidad de Madrid for funding the projects MAT2013-46452-C4-1-R, MAT2013-46452-C4-4-R and S2013/MIT-2753, respectively. Financial support from Universidad San Pablo is also acknowledged.

Notes and references

[1] *Universidad CEU San Pablo, Facultad de Farmacia, Departamento de Química y Bioquímica, Urb. Montepríncipe, Boadilla del Monte, E-28668, Madrid, Spain. Fax: 34 91 3510496; Tel: 34 91 3724728; e-mail: flaga@ceu.es*

[2] *Universidad Complutense de Madrid, Facultad de Ciencias Químicas, Departamento de Química Inorgánica, Ciudad Universitaria s/n, 28040 Madrid, Spain.*

[3] *Universidad Complutense de Madrid, Facultad de Ciencias Químicas, Laboratorio de Altas Presiones, Ciudad Universitaria s/n, 28040 Madrid, Spain.*

1. R. Chen, S. Ren, M. Knapp, D. Wang, R. Witter, M. Fichtner and H. Hahn, *Advanced Energy Materials*, 2015, **5**.
2. R. J. Cava, A. Santoro, D. W. Murphy, S. Zahurak and R. S. Roth, *Journal of Solid State Chemistry*, 1982, **42**, 251-262.
3. R. J. Cava, A. Santoro, D. W. Murphy, S. M. Zahurak and R. S. Roth, *Journal of Solid State Chemistry*, 1983, **50**, 121-128.
4. D. Mariotti, H. Lindstroem, A. C. Bose and K. Ostrikov, *Nanotechnology*, 2008, **19**.
5. F. W. Dampier, *Journal of the Electrochemical Society*, 1974, **121**, 656-660.
6. N. Margalit, *Journal of the Electrochemical Society*, 1974, **121**, 1460-1461.
7. N. Kumagai, N. Kumagai and K. Tanno, *Journal of Applied Electrochemistry*, 1988, **18**, 857-862.
8. G. Guzman, B. Yebka, J. Livage and C. Julien, *Solid State Ionics*, 1996, **86-8**, 407-413.

9. Q. Zhong, J. R. Dahn and K. Colbow, *Physical Review B*, 1992, **46**, 2554-2560.
10. C. G. Granqvist, *Solar Energy Materials and Solar Cells*, 2000, **60**, 201-262.
11. F. Badway, F. Cosandey, N. Pereira and G. G. Amatucci, *Journal of the Electrochemical Society*, 2003, **150**, A1318-A1327.
12. F. Badway, N. Pereira, F. Cosandey and G. G. Amatucci, *Journal of the Electrochemical Society*, 2003, **150**, A1209-A1218.
13. H. Arai, S. Okada, Y. Sakurai and J. Yamaki, *Journal of Power Sources*, 1997, **68**, 716-719.
14. H. Li, G. Richter and J. Maier, *Advanced Materials*, 2003, **15**, 736-739.
15. S. Laruelle, S. Grugeon, P. Poizot, M. Dolle, L. Dupont and J. M. Tarascon, *Journal of the Electrochemical Society*, 2002, **149**, A627-A634.
16. J. Weidlein and K. Dehnicke, *Zeitschrift Fur Anorganische Und Allgemeine Chemie*, 1966, **348**, 278-&.
17. K. Dehnicke and J. Weidlein, *Angewandte Chemie-International Edition*, 1966, **5**, 1041-&.
18. D. W. Murphy, M. Greenblatt, R. J. Cava and S. M. Zahurak, *Solid State Ionics*, 1981, **5**, 327-330.
19. M. V. Reddy, S. Madhavi, G. V. S. Rao and B. V. R. Chowdari, *Journal of Power Sources*, 2006, **162**, 1312-1321.
20. L. Permer and M. Lundberg, *Journal of the Less-Common Metals*, 1989, **156**, 145-159.
21. L. Permer and M. Lundberg, *Journal of Solid State Chemistry*, 1989, **81**, 21-29.
22. C. Bohnke, O. Bohnke and J. L. Fourquet, *Molecular Crystals and Liquid Crystals Science and Technology Section a-Molecular Crystals and Liquid Crystals*, 1998, **311**, 23-29.
23. C. Bohnke, J. L. Fourquet, N. Randrianantoandro, T. Brousse and O. Crosnier, *Journal of Solid State Electrochemistry*, 2001, **5**, 1-7.
24. B. K. Hodnett, P. Permanne and B. Delmon, *Applied Catalysis*, 1983, **6**, 231-244.
25. K. H. Jack and V. Gutmann, *Acta Crystallographica*, 1951, **4**, 246-249.
26. H. G. Bachmann, F. R. Ahmed and W. H. Barnes, *Zeitschrift fuer Kristallographie*, 1961, **115**, 110-131.
27. J. Supel, U. Abram, A. Hagenbach and K. Seppelt, *Inorganic Chemistry*, 2007, **46**, 5591-5595.
28. N. E. Brese and M. Okeeffe, *Acta Crystallographica Section B-Structural Science*, 1991, **47**, 192-197.
29. R. L. Withers, F. J. Brink, Y. Liu and L. Noren, *Polyhedron*, 2007, **26**, 290-299.
30. F. J. Brink, R. L. Withers and L. Noren, *Journal of Solid State Chemistry*, 2002, **166**, 73-80.
31. F. J. Brink, R. L. Withers and J. G. Thompson, *Journal of Solid State Chemistry*, 2000, **155**, 359-365.
32. D. S. Su and R. Schlogl, *Catalysis Letters*, 2002, **83**, 115-119.
33. H. K. Schmid and W. Mader, *Micron*, 2006, **37**, 426-432.
34. M. E. Welk, A. J. Norquist, C. L. Stern and K. R. Poeppelmeier, *Inorganic Chemistry*, 2000, **39**, 3946-+.